SOLUTIONS OF PRANDTL'S BOUNDARY LAYER EQUATIONS USING LINEAR PROGRAMMING AND MAPPINGS

by

GERALD FLYNN

A dissertation submitted to the Graduate Faculty in Mathematics in partial fulfillment of the requirements for the degree of Doctor of Philosophy, The City University of New York.

1979

This manuscript has been read and accepted for the Graduate Faculty in Mathematics in satisfaction of the dissertation requirement for the degree of Doctor of Philosophy.

5/16/79
date

Harry T. Rauch
Chairman of Examining Committee

5/16/79
date

Arden A. Fuld
Executive Officer

Robert Sacksteder

Duane Chavel

Supervisory Committee

The City University of New York

Abstract

SOLUTIONS OF PRANDTL'S BOUNDARY LAYER EQUATIONS USING LINEAR PROGRAMMING AND MAPPINGS

by

Gerald Flynn

Adviser: Professor Harry E. Rauch

A new method of solution to Prandtl's boundary layer equations is proposed and tested for three representative cases. The test flows are: (1) past a flat plate parallel to the stream, (2) past a circular cylinder and (3) linearly retarded flow. For each of these cases we calculate boundary layer thicknesses, velocity profiles and shearing stresses and compare our results to known classical calculations. In the latter two cases, the point of separation is also calculated.

ACKNOWLEDGEMENTS

First, I wish to express my thanks and gratitude to Professor Harry E. Rauch, who suggested the original formulation of this problem, and who allowed me tremendous latitude in re-structuring and re-shaping it into its present form. I thank him also for helping me to develop a perspective on what applied mathematics can and should be, a perspective which will stay with me, I'm sure, until beyond the time this paper has become little more than a dust collector in my bookcase.

To the Mathematics staff at Queensborough Community College, for their support in this past year, I owe a tremendous debt of gratitude. To those running the computer facilities at the CUNY Graduate Center, I give thanks for guidance to a fledgling programmer and for their generous allocation of computer use funds.

Finally, to my wife Jeanne, I owe more than I can express in words. For her patience and understanding during the three years it took to bring this work to its culmination and for "just being there" when she was needed. Finally for her diligence in the monumental task of translating my scrawl into coherent English, I want to publicly express to her all my thanks and my love.

TABLE OF CONTENTS

LIST OF TABLES

LIST OF GRAPHS

1. Introduction. History of the Boundary Layer Equations and a Survey of Earlier Methods of Solution.

Prandtl's Boundary Layer Equations are used to describe the motion of a fluid of low viscosity in the neighborhood of an obstacle residing within the region of the flow. Around the turn of the century, it was generally known that at a reasonable distance from the wall of such an obstacle, the flow behaves essentially as a non-viscous flow and can be described by the theory of potential flow. However, closer to, and at the wall, the equations of potential flow prove incorrect. For example, the "no-slip" condition imposed at the surface by the viscosity are incompatible with potential flow. Thus, the Euler equations:

$$(1) \quad \frac{\partial u}{\partial t} + u\frac{\partial u}{\partial x} + v\frac{\partial u}{\partial y} = -\frac{1}{\rho}\frac{\partial p}{\partial x}$$

$$(2) \quad \frac{\partial v}{\partial t} + u\frac{\partial v}{\partial x} + v\frac{\partial v}{\partial y} = -\frac{1}{\rho}\frac{\partial p}{\partial y}$$

$$(3) \quad \frac{\partial u}{\partial x} + \frac{\partial v}{\partial y} = 0$$

are inadequate to describe the flow near the wall of the obstacle. By taking into account now the viscosity of the fluid, one arrives at the Navier-Stokes equations:

$$(1') \quad \frac{\partial u}{\partial t} + u\frac{\partial u}{\partial x} + v\frac{\partial u}{\partial y} = -\frac{1}{\rho}\frac{\partial p}{\partial x} + \nu\nabla^2 u$$

$$(2') \quad \frac{\partial v}{\partial t} + u\frac{\partial v}{\partial x} + v\frac{\partial v}{\partial y} = -\frac{1}{\rho}\frac{\partial p}{\partial y} + \nu\nabla^2 v$$

$$(3') \quad \frac{\partial u}{\partial x} + \frac{\partial v}{\partial y} = 0$$

In each set of equations above x and y represent curvi-linear co-ordinates parallel and perpendicular to the wall; u and v the velocity components in the x and y directions, respectively; ρ is the density of fluid, p is the pressure, ν is the kinematic viscosity;

∇^2 is the Laplacian operator in x and y and t is the time variable. Certain simplifications have already been built into these equations: we have assumed the density ρ to be constant; this is known as incompressible flow. We have also omitted the "external body forces" which usually appear in the equations. It will further be assumed in the rest of this paper that the flow is time-dependent and so the time derivatives vanish. A complete discussion of these equations may be found in many standard references, Schlichting [9] being one of the better known.

The Navier-Stokes equations have the serious drawback of being so difficult to solve that no general method of solution is known. In 1904, the German scientist L. Prandtl, a pioneer of many important developments in fluid dynamics, developed a new system of equations which bridged the gap between the unacceptable potential (Eulerian) equations and the all but intractable Navier-Stokes equations. Reasoning that the motion of the fluid developed from stationary at the wall of the obstacle to full potential value very rapidly, he introduced the concept of a "boundary layer". Using elementary estimates of all the inertial and viscous terms, Prandtl judiciously eliminated those of smaller orders of magnitude and arrived at his new system of equations which described this transition of the fluid from its zero-value at the wall to its full potential value at some "small distance" away. The words "small distance" are used advisedly and cautiously because there is no clear-cut, well defined distance at which the viscous flow exactly matches the potential flow. The "boundary layer thickness" is experimentally taken to be the distance at which the flow attains 95-99% of full potential and the mathematical treatment is as an asymptotic limit. In the assumed stationary, incompressible form with which we are concerned in this present paper, the form

of the equations are:

$$(4) \quad u\frac{\partial u}{\partial x} + v\frac{\partial u}{\partial y} - U(x)\,U'(x) = \nu\frac{\partial^2 u}{\partial y^2}$$

$$(5) \quad \frac{\partial u}{\partial x} + \frac{\partial v}{\partial y} = 0$$

At this point, for the first time, we discuss boundary and initial conditions. (4), (5) are assumed valid on the set $x \geq 0$, $y \geq 0$. We also have:

$$(6a) \quad u(x,0) = v(x,0) = 0 \qquad x \geq 0$$

$$(6b) \quad \lim_{y \to \infty} u(x,y) = U(x) \qquad x \geq 0$$

$$(6c) \quad u(0,y) = \hat{u}(y) \qquad y \geq 0$$

$U(x)$ represents the potential flow and $\hat{u}(y)$ is known as the "initial profile". Both must be prescribed in order to carry out the solution of the equations. The potential flow is generally well known. The initial profile poses a more fundamental difficulty and is discussed more fully in section 3.

The first genuine solution of these equations was given by Blasius, a doctoral student of Prandtl's, in 1908. He worked on the special case of a flat plate placed parallel to the flow of the stream. Using the principle of similarity (see section 3) he reduced the equations to a single, ordinary differential equation of third order. By considering a combination of a power series solution expanded about the origin and an asymptotic solution at infinity, Blasius derived the first detailed approximate solution of Prandtl's equations.

Blasius also considered other cases of flows. Since that time, many different authors have treated special cases of Prandtl's equations. Most of the earlier solutions were variations on the series expansion

approach. With the development of computers, it became possible to use finite difference approaches to the problem. More recently, too, the Galerkin-Bubnov method has been applied (see Hsu, [5]). The more classical methods are discussed in Schlichting's book (op. cit.) and in Goldstein [2] .

2. Von Mises' Transformation. Formulation of the Linear Programming Problem.

Most methods of solution of the boundary layer equations require certain transformations of both the independent and dependent variables. To put the equations in a form most amenable to the method to be used here, a series of transformations must be used. Starting with equations (4) and (5), we introduce first "non-dimensional" variables by the transformations $u' = {}^{u}/_{U_o}$, $v' = \sqrt{R}\ {}^{v}/_{U_o}$, $x' = {}^{x}/_{L}$, $y' = \sqrt{R}\ {}^{y}/_{L}$ and $U_1 = {}^{U}/_{U_o}$ the equations become:

$$(4') \qquad u' \frac{\partial u'}{\partial x'} + v' \frac{\partial u'}{\partial y'} = U_1 \frac{dU_1}{dx'} + \frac{\partial^2 u'}{\partial y'^2}$$

$$(5') \qquad \frac{\partial u'}{\partial x'} + \frac{\partial v'}{\partial y'} = 0$$

In these transformations, L and U_o are the so called "representative" values of length and velocity, respectively, and $R = U_o L/\nu$ is called the Reynold's number of the flow. The most important advantage of these transformations is that the equations are now independent of the viscosity ν, and so one solution will solve all cases. The form of the boundary and initial conditions are preserved under these transformations.

The important transformation of von Mises will be described in two stages. First, let $\xi = x'$, $\eta = \int_0^{y'} u'(x',t)\, dt$ be the new independent variables and let $\varphi(\xi, \eta) = u'(x'(\xi,\eta), y'(\xi,\eta))$ and $U_2(\xi) = U_1(x')$. Then the equations (4'), and (5') reduce to:

$$(6) \qquad \varphi \frac{\partial \varphi}{\partial \xi} = U_2 \frac{dU_2}{d\xi} + \frac{\partial}{\partial \eta}\left(\varphi \frac{\partial \varphi}{\partial \eta}\right)$$

with the boundary conditions becoming:

(7a) $\varphi(\xi,0) = 0$

(7b) $\lim_{\eta\to\infty}\varphi(\xi,\eta) = U_2(\xi)$

(7c) $\varphi(0,\eta) = \hat{\varphi}(\eta) = u'(y'(0,\eta))$

Finally letting

$$z(\xi,\eta) = U_2^2(\xi) - \varphi^2(\xi,\eta)$$

we obtain:

$$(8)\quad \frac{\partial z}{\partial \xi} = \sqrt{U_2^2(\xi) - z(\xi,\eta)}\ \frac{\partial^2 z}{\partial \eta^2}$$

with the boundary conditions:

(9a) $z(\xi,0) = U_2^2(\xi)$

(9b) $\lim_{\eta\to\infty} z(\xi,\eta) = 0$

(9c) $z(0,\eta) = \hat{z}(\eta) = U_2^2(0) - \hat{\varphi}^2(\eta)$

Equation (8) bears a superficial resemblance to the one dimensional heat equation, but the conductivity term is replaced by the variable, non-linear term $\sqrt{u^2-z}$.

This equation is not without it's disturbing features. If we let $\eta\to 0$, we see that there is a singularity at $\eta = 0$, which could be fatal to a numerical approximation approach. We will now put the equation into its final form for the proposed method. It will be necessary to transform the region in which the equation, boundary and initial conditions are defined into one which is bounded in both its independent variables. This could have been done in several ways; algebraic transformations have proved superior to straight truncation or exponential transformations in previous studies (see Grosch and Orszag, [3]).

Set $x_1 = \xi$ and $y_1 = (\eta - \alpha)/(\eta + \alpha)$. Here $\alpha > 0$ is a constant which is chosen to control the error due to the mapping. Several trial runs were made using different values of α and $\alpha = 10$ seemed to be the "best" choice in the cases considered here. It seems entirely plausible that α could be chosen as a function of x_1, but as no natural choice of such a function was evident this was not attempted here. The mapping transforms the interval $0 \leq \eta < \infty$ onto $-1 \leq y_1 \leq 1$ in a one to one fashion. We will continue to use z as the dependent variable and U_2 for the potential flow. Making changes of variable in the usual way and using the result $\partial y_1/\partial \eta = (1-y_1)^2/2\alpha$ we obtain the final form of the equations:

$$(10) \quad \frac{\partial z}{\partial x_1} = \sqrt{U_2^2(x_1) - z(x_1,y_1)} \left[\frac{(1-y_1)^4}{4\alpha^2} \frac{\partial^2 z}{\partial y_1^2} - \frac{(1-y_1)^3}{2\alpha^2} \frac{\partial z}{\partial y_1} \right]$$

with the boundary and initial conditions:

$$(11a) \quad z(x_1,-1) = U_2^2(x_1)$$

$$(11b) \quad z(x_1,1) = 0$$

$$(11c) \quad z(0,y_1) = U_2^2(0) - \hat{\varphi}^2(y_1) \equiv \hat{z}(y_1)$$

Here, of course, $-1 \leq y_1 \leq 1$ and $0 \leq x_1 \leq X$. The choice of X depends on the problem. We considered three test cases in this paper. For the flat plate at zero incidence, the usual theoretical convention is to take the plate as being infinite in length. For computational purposes, we took X = 1, although any value would have been acceptable. For the flow about a cylinder and the so-called linearly retarded flow, we continued the solution up to the point of separation. These problems will be completely discussed in subsequent sections. Another fact that should be observed is that the wall is located

at $y_1 = -1$, rather than at 0, as is usually the case. With all of this background behind us, we are now in a position to discuss the linear programming formulation of the solution. For convenience of the notation, the subscripts on x, y and U will be dropped in the rest of this discussion. The idea of solving a parabolic partial differential equation by linear programming was developed by J. Rosen ([8]). We start by considering an equation of the form:

$$(12) \qquad z_x = \hat{N}(x,y,z,z_y,z_{yy}) \qquad \begin{cases} 0 \leq x \leq X \\ -1 \leq y \leq 1 \end{cases}$$

with conditions:

$$(13a) \qquad z(x,-1) = U^2(x)$$

$$(13b) \qquad z(x,1) = 0 \qquad \left\{ \; 0 \leq x \leq X \right.$$

$$(13c) \qquad z(0,y) = \hat{z}(y) \qquad -1 \leq y \leq 1$$

where $\hat{N}$ is a non-linear operator in general, and that operator on the right hand side of (10) in this particular case. We select grids in both the x and y directions:

$0 = x_o < x_1 < \cdots < x_K = X$ and $-1 = y_o < y_1 < \cdots < y_M = 1$ and an approximate value for z by the series $\bar{z}(x,y) = \sum_{j=0}^{N} A_j(x)\, T_j(y)$, where $T_j(y)$ stands for the j^{th} Chebyshev polynomial. The functions $A_j(x)$ are to be determined by the process. Starting at $x = x_o$ we match $\bar{z}(x_o,y)$ to z(y) by the following scheme:

Let $w_{oj} = A_j(x_o)$. We now select the values w_{oj} so that $\bar{z}(x_o,y_k) = \hat{z}(y_k)$ for $k = 0$ and $k = M$ and so as to minimize the error

$$E = \max_{1 \leq k \leq M-1} \left| \bar{z}(x_o,y_k) - \hat{z}(y_k) \right|$$

at the remaining points of the y-grid. In other words,

we attempt to match the series exactly to the boundary data and to obtain the best fit in the mini-max sense at the remaining grid points. To see the actual linear programming aspect of this situation, we consider the variables: $y_o, y_1, \cdots, y_m, \gamma$; and the following sets of constraints:

$$\text{(14a)} \quad \hat{z}(y_k) \leq \sum_{J=0}^{N} A_{jk}\, w_{oj} + \gamma$$

$$\text{(14b)} \quad -\hat{z}(y_k) \leq \sum_{J=0}^{N} -A_{jk}\, w_{oj} + \gamma \qquad \left\{ 1 \leq k \leq M-1 \right.$$

$$\text{(14c)} \quad \sum_{J=0}^{N} T_j(-1)\, w_{oj} = \hat{z}(-1)$$

$$\text{(14d)} \quad \sum_{J=0}^{N} T_j(1)\, w_{oj} = \hat{z}(1)$$

Equations (14a) and (14b) are easily seen to be equivalent to:

$$\text{(14e)} \quad -\gamma \leq \sum_{J=0}^{N} A_{jk}\, w_{oj} - \hat{z}(y_k) \leq \gamma$$

In these equations $A_{jk} = T_j(y_k)$. It is clear that we must choose the w_{oj} in order that the constraints be satisfied and γ is as small as possible. This can be formulated in matrix form as:

$$\text{(14f)} \quad \min \left\{ BY^T \,\middle|\, A^T Y \geq C \right\} \text{ where}$$

$$B = \underbrace{(0, 0, \cdots, 1)}_{M+1 \text{ entries}}, \quad Y = (y_1, \cdots y_M, \gamma)$$

$$C^T = (\hat{z}(y_1), \cdots \hat{z}(y_M), \hat{z}(-1), \hat{z}(1), -\hat{z}(y_1), \cdots -\hat{z}(y_M), -\hat{z}(-1), -\hat{z}(1))$$

and $A = \left(\begin{array}{c|cc|c|cc} A_{jk} & T_j(-1) & T_j(1) & -A_{jk} & -T_j(-1) & -T_j(1) \\ \hline 1 \cdots 1 & 0 \cdots 0 & & 1 \cdots 1 & 0 \cdots 0 & \end{array}\right)$

Actually, (14f) is generally called the dual problem of a related linear programming problem:

$$(14g) \qquad \max \left\{ C^T X \,\middle|\, AX = B \right\}$$

where equality is chosen in order to allow non-positive values in the dual. All of the details of this are found in Rosen's paper and details on the linear programming may be found in Hadley ([4]). Most of the notation here follows Rosen's, except that certain parts have been specialized for our problem.

At this point, we have merely approximated the initial profile. The method may be applied successively to continue the solution to $x = X$. We assume that $w_{ij} = A_j(x_i)$ has already been found, and procede to compute $w_{i+1,j}$. First, we let $h_i = x_{i+1} - x_i$ and then we may approximate:

$$A_j'(x_i) \approx \frac{A_j(x_{i+1}) - A_j(x_i)}{h_i} = \frac{w_{i+1,j} - w_{ij}}{h_i}$$

then:

$$(15) \qquad \frac{\partial \bar{z}}{\partial x} \approx \sum_{J=0}^{N} \frac{w_{i+1,j} - w_{ij}}{h_i} T_j(y) = \hat{N}(x_i, y, z, z_y, z_{yy})$$

or:

$$(16) \qquad \sum_{J=0}^{N} w_{i+1,j} T_j(y) = \sum_{J=0}^{N} w_{ij} T_j(y) + h_i \hat{N} \Big|_{x=x_i}$$

In the same spirit as before, we choose the $w_{i+1,j}$ so that:

$$(17a) \qquad \sum_{J=0}^{N} w_{i+1,j} T_j(-1) = U^2(x_i)$$

$$(17b) \qquad \sum_{J=0}^{N} w_{i+1,j}\, T_j\,(1) = 0$$

and to minimize the error expression:

$$(18) \qquad \left| \sum_{J=0}^{N} w_{i+1,j}\; A_{jk} - \sum_{J=0}^{N} w_{ij}\, A_{jk} - h_i\, \hat{N} \right|$$

The formulation of this as a linear programming problem is identical to that in the initial profile. The actual problem was run on the City University of New York's IBM 370 computer. The International Mathematics and Statistical Library (IMSL) has available for computer users prepackaged programs related to many problems in optimization. For this problem, the package ZX3LP (see IMSL manual, [6]) was used. The main advantage of using a prepackaged program here is that such a program has been tested for reliability and accuracy with controls to guard against roundoff problems, etc. A disadvantage is a reduction of flexibility on the user's part. In this case, the fact that matrix C varies only slightly from one step to the next may be exploited so that the entire process need not be repeated at each change in x. However, the program being used does not seem to allow that option, which means, perhaps, a slight increase in computer running time. It would appear that the advantages outweigh the disadvantages, especially since no program ran more than about 6 minutes, with 3 minutes being closer to the typical value.

It was mentioned earlier in this section that equation (8) and consequently (10) experience a singularity at y = -1. This present procedure circumvents the problem merely by not requiring the match of the series to the p.d.e. at that point, replacing that condition by the exact match of the boundary condition there. Although Rosen's paper did not deal with the possibility of singularities within the region, the highly accurate solutions in most cases would seem to validate the use

of this technique, at least as a first approximation.

We will now conclude this section with an important comment on the functions $A_j(x)$. The formulation we have been using defines them only at a discrete set of points $x_o < x_1 < \cdots < x_k = X$. It is generally assumed in series expansions of the type we have been using that such "co-efficient" functions are continuous. It did not seem necessary for this problem to do so, but the functions $A_j(x)$ could be approximated by interpolating polynomials using the points already selected.

3. The Initial Profile. The Case of a Flat Plate at Zero Incidence.

The Prandtl system of partial differential equations (4),(5) together with conditions (6a,b) are not, in general, sufficient to give us a well-posed problem. In order to determine uniquely a solution to this system, the additional boundary conditions (6c) must be considered. This is analogous, for example, to one-dimensional heat flow, where it is necessary to prescribe the flow of heat at time zero. In boundary layer theory, this initial value is called the "initial profile". It is generally taken to be the pre determined value of the flow at some value of x, usually 0. The problem then becomes to describe $u(x,y)$ for $x > 0$. So, in a sense, in solving Prandtl's equations we are tracing the further development of a given non-viscous flow (the initial profile) together with a given, associated external flow (or pressure gradient, see section 6) as the fluid moves downstream in the neighborhood of an obstacle. An important paper by J. Serrin ([10]) gives some discussion of this problem and provides references for existence and uniqueness theory. Nickel ([7]) also treats this problem and traces some of the historical development of the boundary layer equations in the first three quarters of a century since their formulation.

The problem facing one attempting to solve numerically the Prandtl equations is somewhat different. It is acknowledged that some type of initial function is needed; the significant question becomes how to choose such a function. There is nothing in the theory of fluid mechanics to suggest an appropriate profile which would describe the onset of boundary layer development. The approach of Blasius, and many writers who followed in the same spirit seems almost a deliberate attempt to avoid an assignment of such an initial profile. The idea of "similarity flow" was applied in several cases

and proved a useful simplifying device.

Similarity is basically an assumption that the flow changes from one value of x to another only by a change in scale of the y-variable; generally one takes $u(x,y) = g(\eta)$ where $\eta \sim y/\sqrt{x}$ with the proportionality constant being determined by the viscosity and potential velocity of the flow. This device reduces the partial differential equations (4),(5) to a single, ordinary differential equation. The assumption of similarity is valid where $U(x) = ax^m$ is the external flow. A most significant result due to Serrin (op. cit.) proves that if $m \geq 0$, then no matter what initial profile one chooses, any solution to Prandtl's equations approaches the similarity solution asymptotically as $x \longrightarrow \infty$.

From a strictly mathematical point of view, any function will do, allowing for some simple continuity and differentiability conditions. However, there is no guarantee that this will lead one to a realistic flow for the region of interest. Were the information available, one could construct a function based on an experimentally determined initial profile, but in the absense of this or anything else more definitive it almost seems best to simply let $u(0,y) = U(0)$, where $U(x)$ is the given potential velocity. This may be too arbitrary for most theoretical work (see Serrin, op. cit.) and may cause computational problems because of the discontinuity at the wall (the "no-slip" condition $u(x,0) = 0$ is violated at $x = 0$ unless $U(0) = 0$). Nickel (op.cit) stresses the importance of continuity in $\hat{u}(y)$ and the related problem of letting $U(0) = 0$. Furthermore, a numerical method such as that used here requires that $\hat{u}(y)$ have continuous second derivatives in order to guarantee a solution. The numerical solver's problem thus becomes one of obtaining an initial profile which is both physically plausible and sufficiently smooth to allow the chosen numerical scheme to work.

For the flat plate placed parallel to the stream (referred to as "zero incidence"), the potential flow is a constant U_o and because of the non-dimensionalization of section 2, this constant may as well be taken as 1. We will develop the initial profile as a series of approximations. First, we take:

$$(19) \quad \hat{U}(y) = \begin{cases} 1 & \text{if } y > 0 \\ 0 & \text{if } y = 0 \end{cases}$$

This profile is seen to match both the main stream velocity as $y \to \infty$ as well as the "no-slip" condition on the plate itself. We now trace the development of this profile through the series of transformations used and in the final set of variables the profile takes the form:

$$(20) \quad \hat{Z}_1(y_1) = \begin{cases} 1 & \text{if } y_1 = -1 \\ 0 & \text{if } -1 < y_1 \leq 1 \end{cases}$$

Since this function is not continuous, we try to fit a twice continuously differentiable curve to this data and arrive at:

$$(21) \quad \hat{Z}(y_1) = \begin{cases} \left(\dfrac{y_1 + 0.81}{-0.19}\right)^3 & \text{if } -1 \leq y_1 \leq -0.81 \\ 0 & \text{if } -0.81 < y_1 \leq 1 \end{cases}$$

This choice has sufficient smoothness throughout $[-1,1]$ and is a reasonable match for the data. The choice of -0.81 as the zero of the cubic branch is admittedly arbitrary. However, the grid in y was in uniform increments of 0.05 and this enabled the series match to be fairly smooth. The accuracy of the approximation to the profile depends greatly on the number of modes in the approximation series. Referring back to the discussion of the linear programming scheme, the variable γ is, at this stage, actually a measure of the error of the approximation. From general linear

programming theory, in an N mode approximation, this maximum error is attained exactly N-1 times. The size of this error decreases as the number of modes increases. For a six mode approximation, this error is 0.1693, which is quite large. The error sizes for 10 and 16 modes are 0.0132 and 0.0020, respectively. Table 1 and graph 1 illustrate these approximations quite nicely. Some of the computations here were done on a hand calculator, which is tedious but nevertheless feasible once the co-efficient values are known. While in view of Serrin's Theorem on similarity flows, the appropriateness of our choice for initial profile need not be at issue, we will see that the subsequent development of the velocity profile becomes reasonably uniform quite quickly. The rest of the discussion of the flat plate solution will be presented in the next two sections.

Table 1. Initial Profiles: Z_N represents the N mode approximations to z.

Y	Z(y)	$Z_6(y)$	$Z_{10}(y)$	$Z_{16}(y)$
-1.0	1.000	1.000	1.000	1.000
-0.8	0.0	-0.0803	-0.0132	-0.0020
-0.6	0.0	-0.1207	0.0121	-0.0020
-0.4	0.0	0.0845	-0.0132	0.0016
-0.2	0.0	0.1693	0.0050	-0.0011
0.0	0.0	0.0706	0.0096	0.0010
0.2	0.0	-0.0976	-0.0120	-0.0010
0.4	0.0	-0.1693	-0.0001	0.0008
0.6	0.0	-0.0520	-0.0126	0.0003
0.8	0.0	0.1480	-0.0132	-0.0020
1.0	0.0	0.0000	0.0000	0.0000

Graph 1. Initial Profiles.

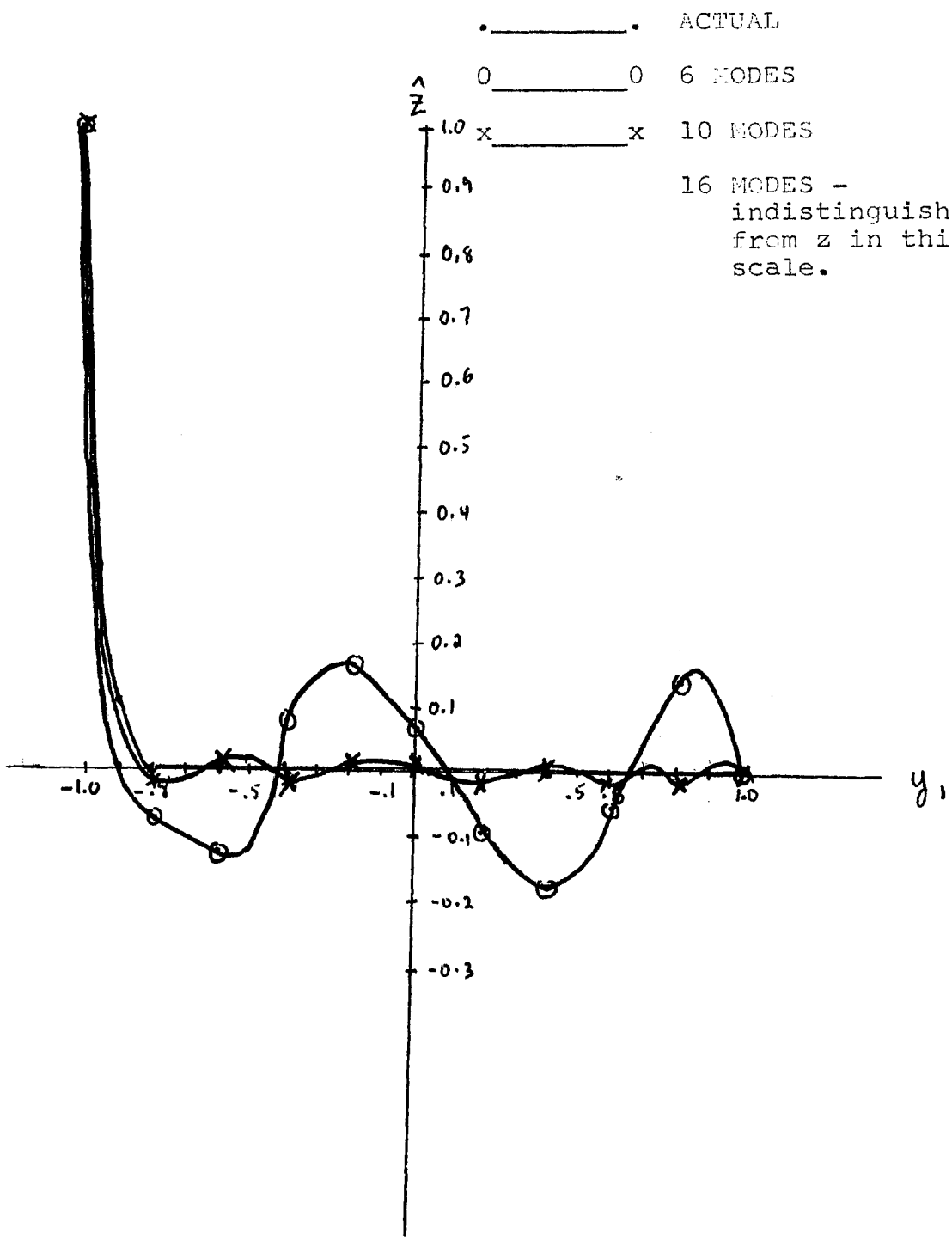

4. Results for the Plate - Velocity Profiles and Boundary Layer Thickness.

The general discussion of the linear programming was given in section 2. The parameters α and h_i remain to be chosen. This type of selection is somewhat subjective. The "objective function" which was minimized by this method is actually the variable γ, which serves as the error in approximating the left hand side to the right hand side of (12). The values of h_i (which we will refer to as the "time step" in analogy with the heat equation) and α (referred to as a "truncation number") were initially arrived at by running the procedure from $x = 0$ to $x = .02$, using different time steps and truncation numbers. The most accurate results appeared to be when $\alpha = 10$ and $h = 0.001$.

In this type of problem, one must also be cognizant of the amount of computer time involved. For example, to procede from $x = 0$ to $x = 1$ in increments of .001 would require 1000 time steps. This would require 1000 calls to the subroutine ZX3LP for a simplex procedure which involves an inversion of a large order matrix and a host of other time consuming routines. As was mentioned before, greater flexibility in using the simplex package would have given us some increased speed, but none of the times were too great for any of our trials. What did help us here was the property of similarity. Taking the reasonable assumption that the flow is stabilizing to the similarity profile, we chose to periodically "update" the time step h. From $x = 0$ to $x = .02$, $h = 0.001$; for $0.02 < x \leq 0.10$, $h = 0.002$; for $0.10 < x \leq 0.50$, $h = 0.004$ and for $0.50 < x \leq 1.0$, $h = 0.005$. In this way, the procedure took only 260 time steps and subroutine calls. The time varied as the number of modes: for $N = 6$, the time was about 0.45 minute; for $N = 10$, slightly over 1 minute and for $N = 16$, slightly over 3 minutes. One curious fact we observed was that

immediately after a change in the time step the error increased slightly and then started to decrease again fairly rapidly.

After the initial step, the error dropped dramatically in all three cases. For example, in the 16 mode case, the error at the initial station was 0.2×10^{-2} and then at x = .001 the error dropped to 0.128×10^{-4}. This error increased slightly for the next few steps, reaching a maximum of about 0.92×10^{-4} and decreased thereafter except for the time step change phenomenon. At the end of the region considered (x = 1) we had an error value of -0.136×10^{-5}. For the 10 and 6 mode cases the results are not quite so good, but they are reasonable. The 10 mode approximation error is generally in the neighborhood of 10^{-4} and the 6 mode error about 0.5×10^{-3} with improvement of about a power of 10 near the end of the flow region considered.

Table 2, which appears at the end of this section, gives us a superb analysis of this situation. This table lists the values of the co-ordinate functions for four different values of x. At each x value, the co-efficient functions for 6, 10 and 16 modes may be compared. As one might expect, the 16 mode expression shows the most rapid convergence since its co-efficient values approach 0 faster than the other two cases. Another interesting observation is made by comparing the values of a particular A; for a particular x. For example, $A_o(.75) = .1709, .1715, .1715$ in the 6,10 and 16 mode cases, respectively. Similar comparisons could be made for other cases, too, with this type of strong agreement exhibiting itself for x values even only slightly higher than 0. This is a strong indication of stability - the 10 mode case really does appear to be a truncated form of the 16 mode case.

One of the results one would be interested in when solving Prandtl's equation is the velocity profile u(x,y).

To relate this to $z(x_1,y_1)$, which is what we actually solve for here, we first set $\varphi(\xi,\eta) = \sqrt{U^2(\xi) - z(\xi,\eta)}$ where $\eta = \frac{y-\alpha}{y+\alpha}$. This really amounts to reversing the transformations discussed in section 2. However, if one wishes the velocity profile in the original (non-dimensional) variables (x',y') it becomes necessary to invert the von Mises transformation: $\eta = \int_0^{y'} u'(x',t)dt$. The inverse of this transformation gives us:

$$y' = \int_0^{\eta} \frac{1}{u'(\xi, T)}\, dT$$

The difficulty here is, of course, that this integral is singular at T=0, and is difficult to solve numerically. Another quantity of interest is the so-called boundary layer thickness. In this paper we will take it to be that value of y' at which u'(x',y') achieves 99% of $U_1(x')$. It may be seen that in the final co-ordinates the boundary layer thickness becomes that value of y_1 at which $z(x_1,y_1) = 0.02\, U_1^2(x_1)$. We call this value y_1^* and the corresponding value in the original co-ordinates δ. Combining all the transformation inversions together, we obtain the relation:

$$(22) \quad \delta = \int_{-1}^{y_1^*} \frac{2\alpha\, dw}{(1-w)^2 \sqrt{U_1^2(x_1) - z(x_1,w)}}$$

The integration of (22) was accomplished in the following way. For a given value of x_1, the series for $z(x_1,y_1)$ was summed for y = -1 in increments of 0.01 until y_1^* was approximately reached. That is, we stopped at the first value of y_1 for which $z(x_1,y_1) < 0.02\, U_1^2(x_1)$. We were not particular about the exact value of y_1^* since the definition of boundary layer thickness is somewhat

subjective anyway. We then approximated (22) by evaluating the integral with the lower limit first -0.97 and then -0.96. These were evaluated by the trapezoidal rule, using $\Delta = 0.005$. The two values were compared mainly for the sake of checking on errors due to truncation. In each case, the integration from -0.97 was taken to be the value of δ we desired.

For the case of the flat plate it was very easy to compare these results with classical values. Based on Blasius' solution, the boundary layer thickness is given by $\delta(x) = 4.9\sqrt{x}$ (see Batchelor [1] and Goldstein, op. cit.). The results of these integrations and the comparison of our results to those of classical methods, are given in Table 3 and graph 2. Only the 16 mode case was used for these calculations.

The comparisons are fairly good. The boundary layer thickness is really only a convenient concept and does not represent an actual physical "layer" or region in the stream of flow. The approximate orders of magnitude are clearly the same and this is all that should really matter. These estimated boundary layer thicknesses indicate that our proposed model does describe a flow which behaves very much in the way that is expected and gives strong evidence to the validity of this model.

Comparison of Co-ordinate Functions in Different Modes.

Flat Plate Case.

Table 2a

	x = 0.0			x = 0.40		
	M=6	M=10	M=16	M=6	M=10	M=16
A_0	.1163	.0910	.0900	.1211	.1493	.1498
A_1	-.1680	-.1755	-.1775	-.1846	-.2846	-.2832
A_2	.2147	.1667	.1651	.2180	.2364	.2371
A_3	-.1279	-.1465	-.1490	-.1346	-.1755	-.1743
A_4	.1690	.1272	.1263	.1609	.1078	.1085
A_5	-.2041	-.1001	-.1031	-.1809	-.0553	-.0535
A_6		.0785	.0782		-.0154	-.0156
A_7		-.0529	-.0560		-.0001	-.0039
A_8		.0365	.0362		-.0090	-.0096
A_9		-.0249	-.0254		.0154	.0075
A_{10}			.0093			-.0032
A_{11}			-.0016			-.0000
A_{12}			-.0020			.0013
A_{13}			.0039			-.0010
A_{14}			-.0032			.0004
A_{15}			.0038			.0005

Comparison of Co-ordinate Functions in Different Modes.

Flat Plate Case.

Table 2b

	x = 0.75			x = 1.0		
	M=6	M=10	M=16	M=6	M=10	M=16
A_0	.1709	.1715	.1715	.1808	.1827	.1826
A_1	-.3282	-.3185	-.3184	-.3491	-.3356	-.3356
A_2	.2473	.2529	.2528	.2514	.2588	.2584
A_3	-.1732	-.1672	-.1675	-.1721	-.1604	-.1609
A_4	.0817	.0865	.0867	.0678	.0738	.0737
A_5	.0013	-.0275	-.0279	.0212	-.0146	-.0156
A_6		-.0033	-.0033		-.00995	-.00996
A_7		.0106	.0121		.0123	.0128
A_8		-.0076	-.0089		-.0053	-.0064
A_9		.0026	.0028		-.0017	.0002
A_{10}			.0009			.0019
A_{11}			-.0016			-.0012
A_{12}			.0008			.0001
A_{13}			.0002			.0005
A_{14}			-.0004			-.0004
A_{15}			.0002			-.0002

Table 3. Boundary Layer Thickness (Flat Plate)

y : boundary layer thickness in final co-ordinates (16 mode expansion).

δ_{16} : equivalent value in original co-ordinates.

δ_c : boundary layer thickness based on Blasius' results.

$u(x, \delta_{16})$: value of velocity profile at the edge of the boundary layer.

x	0.0	0.2	0.4	0.6	0.8	1.0
y	-0.85	-0.72	-0.64	-0.59	-0.54	-0.50
δ_{16}	0.78	1.85	2.60	3.14	3.70	4.17
δ_c	0.0	2.19	3.10	3.80	4.38	4.90
$u(x, \delta_{16})$	0.9943	0.9908	0.9914	0.9900	0.9908	0.9910

Graph 2. Boundary Layer Thickness

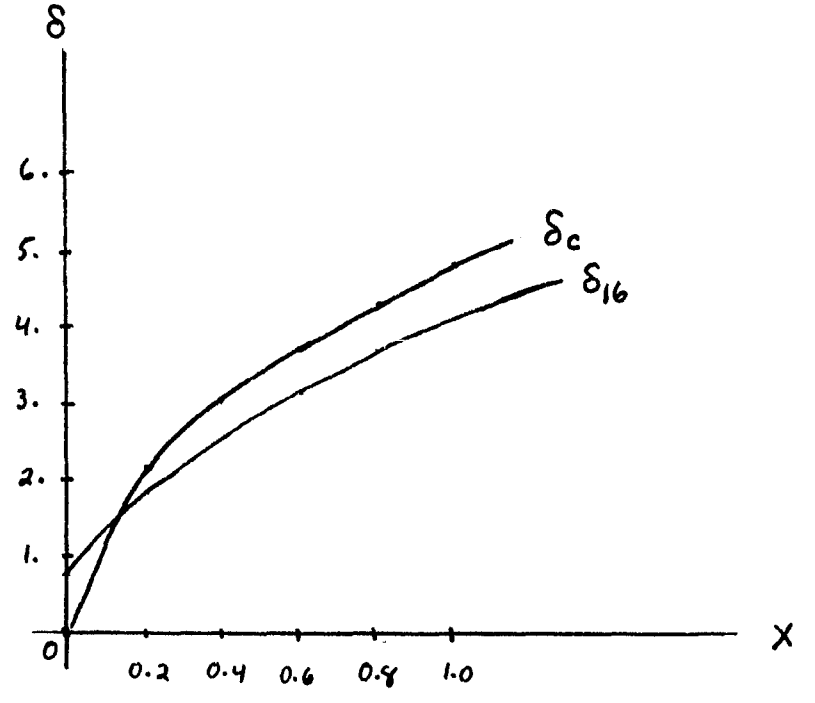

5. Results for the Plate- Shearing Stress Profiles.

An important result to be obtained from the solution of Prandtl's equation is the shearing stress along the wall of the obstacle. The value of the stress is given in the original (dimensional) co-ordinates by $\tau_c(x) = \mu(\frac{\partial u}{\partial y})_{y=0}$. By using the change to non-dimensionalized variables of section 2, we obtain the non-dimensional stress function:

$$(23) \qquad \tau_o(x') = \frac{\tau_c(x)}{\rho \nu^{1/2} U_o^{3/2} / L^{1/2}}$$

Next, by applying successively the von Mises and the algebraic truncation we obtain the relations:

$$(24) \qquad \tau_o(x') = -\tfrac{1}{2} (\frac{\partial z}{\partial \eta})_{\eta=0} = -\frac{(1-y_1)^2}{4\alpha} (\frac{\partial z}{\partial y_1})_{y_1 = -1}$$

$$(25) \qquad \tau_o(x_1) = -\frac{1}{\alpha} (\frac{\partial z}{\partial y_1})_{y_1 = -1}$$

These results are quite general. In particular, using the series

$$z(x_1, y_1) = \sum_{j=0}^{N} A_j(x)\, T_j(y)$$

and the fact that

$$T_j'(-1) = (-1)^{j+1} j^2 ,$$

we can obtain a series for $\tau_o(x_1)$:

$$(26) \qquad \tau_o(x_1) = \sum_{j=1}^{N} (-1)^{j+1} j^2 A_j(x)$$

For the case of the plate, we have Blasius' solution as a basis of comparison. From Blasius' solution, we know that for the plate

$$\tau_c(x) = \tfrac{1}{4} \alpha_1 \rho U_o (\nu U_o / x)^{1/2} , \qquad \text{where}$$

$\alpha_1 = 1.32824$ (see Goldstein, op. cit.).

These results can be transformed to compare to (23):

$$(27) \qquad \tau_o(x') = \frac{\tau_c(x)}{\rho \nu^{1/2} U_o} 3/2 / L^{1/2}$$

$$(28) \qquad \tau_o(x') = \frac{\alpha_1}{4} \frac{1}{\sqrt{x'}}$$

Since x' and x_1 are actually the same variable, we may now compare (26) and (28) directly. The results are reasonable but not really as nice as one might like. We have provided both a table and a graphical comparison of the classical results (28) to the series (26) for all three cases considered. The 6 mode case is uniformly poor; the 10 and 16 mode cases are slightly better. Although it is difficult to ascertain exactly why the convergence is poor, a partial explanation may lie in the fact that differentiation of the Chebyshev polynomials introduce a factor of j^2 into the series - a factor which can significantly slow the rate of convergence. Table 4 and graph 3 should be referred to at this time. In terms of relative error, each approximation improves as x increases, all achieve roughly a 4% error for $x > .9$. For the scale that we had to use for the graph, the results look reasonable close in all three cases.

Table 4: Stress Profiles

x	$\mathcal{T}_0(x)$	$\mathcal{T}_6(x)$	$\mathcal{T}_{10}(x)$	$\mathcal{T}_{16}(x)$
0.0		0.9985	1.6474	1.4995
0.1	1.0501	0.8525	0.8469	0.7964
0.2	0.7425	0.7405	0.6716	0.6897
0.3	0.6063	0.6505	0.5379	0.5886
0.4	0.5250	0.5783	0.4650	0.5046
0.5	0.4696	0.5201	0.4202	0.4455
0.6	0.4287	0.4725	0.3896	0.4047
0.7	0.3969	0.4325	0.3666	0.3761
0.8	0.3713	0.3988	0.3482	0.3542
0.9	0.3500	0.3703	0.3328	0.3365
1.0	0.3321	0.3459	0.3193	0.3221

Graph 3 - Stress Profiles

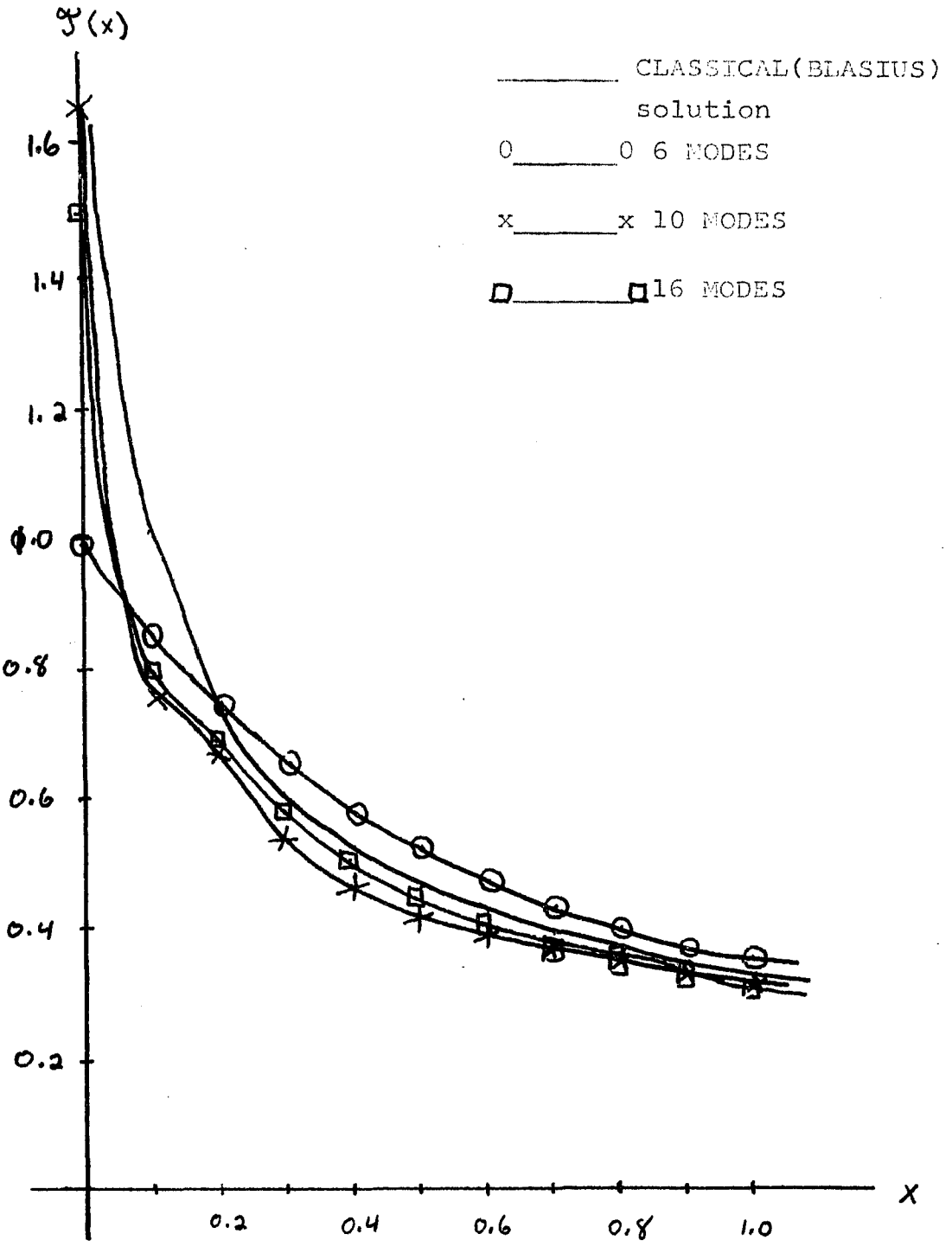

6. Flow about a Circular Cylinder. Separation

Although the results for the plate flow are encouraging, the simplicity of that problem does not provide a very great challenge to the linear programming method. A case which does provide us with a little more challenge is that of flow past a right circular cylinder. The difficulty here is due to a mainstream velocity which is at first increasing and later decreasing. Furthermore, the deceleration is directly related to an increasing pressure gradient near the wall which retards the motion of the fluid and causes separation- the phenomenon in which the fluid actually becomes detached from the wall. Beyond separation the motion of the fluid changes radically; the boundary layer thickens rapidly to the extent that the simplifying assumptions of Prandtl's equations are no longer valid. At the point of separation, the shearing stress at the wall is zero; this provides us with a relatively easy way of detecting that point. Using equation (26), we may compute the stress value at each time step. This may be done by the addition of a very simple routine into our computer program; it does not add significantly to the running time. As soon as we observe $\mathcal{T}_o(x) \leq 0$, the process is stopped. Since we have $\mathcal{T}_o(x_k) > 0$, $\mathcal{T}_o(x_{k+1}) < 0$, we may find the actual separation point x_s by interpolation. This will be carried out in detail in the next section.

The main details of the linear programming formulation of the problem correspond to the general set-up described in section 2. All that is needed here is the assignment of appropriate external and initial station flows.

The choice of the external flow will be taken from inviscid flow, although that is not the only suitable choice in this case. The usual definition of the independent variable x is distance measured along the

surface of the cylinder from point A (refer to figure below). If we let a represent the radius of the cylinder,

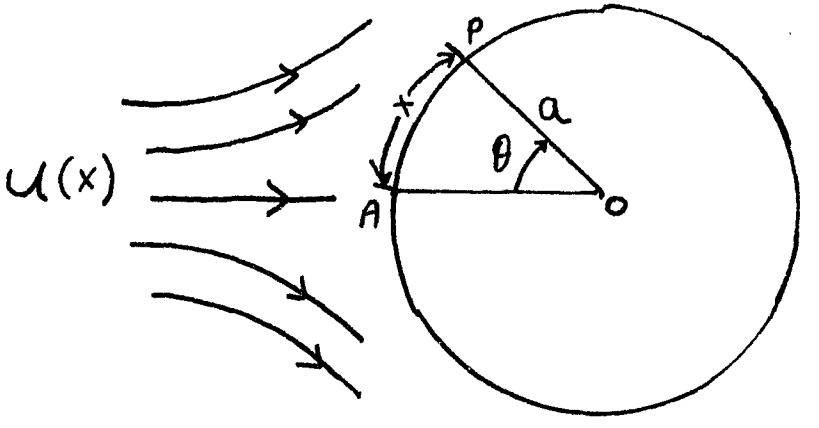

the main stream (inviscid) velocity is given by $U(x) = 2U_o \sin(\frac{x}{a})$, with U_o representing the free "undisturbed" velocity of the stream. By using the non-dimensional lengths $\frac{x}{a}$ and $y\sqrt{R}/a$, as discussed in section 2, we may really consider the variable θ, which is the angular displacement from A to P, instead of the length x as one of our independent variables. In its non-dimensional form, we have $U(\theta) = 2\sin\theta$ for the external flow velocity.

The problem of an initial profile is actually much easier and more natural here than in the case of the plate. For flow about the cylinder, we have at A the condition of "stagnation" - the flow has zero velocity at that point. Instead of attempting to describe an initial flow for $\theta = 0$, we use the condition of stagnation as our initial flow condition for this problem. Actually, we set $u(0,y) = 0$ for $y \geq 0$; this is consistent with most classical approaches to the problem (see Schlichting, op. cit. for a discussion of some of the classical variations on Blasius' solution to this flow). From this point on, the solution proceeds identically to the previous case. We move in steps of 0.005; this step size proved more than adequate to give the flow with a

high degree of accuracy all the way up to separation. Again, we took α = 10 and used 40 grid points in y. Two cases were considered here - 16 modes and 20 modes in the series approximation.

7. Results for the Cylinder.

Generally speaking, the results for the cylinder were quite good. Stagnation could be matched exactly and this fact started the whole process off quite strongly and accurately. In the 16 mode approximation, the error fluctuated somewhat between a low of 0.6×10^{-6} at $x = 0.005$ to a high of 0.65×10^{-4} near separation ($x = 1.945$). For most of the region, the error stayed in the 10^{-5} range, but as separation became imminent it exhibited a rapid relative increase from 0.446×10^{-4} at $x = 1.9$ to the aforementioned 0.65×10^{-4} at $x = 1.945$. This change, which is about 45%, can be, at least in part, attributed to the growing instability of the flow as separation approaches. To determine the point of separation, we observe that $\gamma_o(1.940) = 0.101957 \times 10^{-1}$ and $\gamma_o(1.945) = -0.179794 \times 10^{-1}$. Using the simple device of linear interpolation, we estimate that separation takes place at $x = 1.9418$. This is about 111^o from stagnation, a result which compares favorably to 108.8^o as is found by Blasius' solution (see Schlichting). The entire process required 389 time steps and ran a total of 3.25 minutes.

The profile for the shearing stress is given in graph 4. Compared with the classical values from Schlichting, we see that this method consistently underestimates the actual stress for most of the region except, ironically very close to separation.

The 20 mode approximation fared only slightly better. In advancing from one x value to the next, again in steps of 0.005, the error was more consistently in the $10^{-6} - 10^{-7}$ range and even near separation it was approximately 4×10^{-6}. In this case, the separation point was found to be $x = 1.9339$ (110.8^o from the forward stagnation point). Again referring to graph 4, we see

that the stress is also underestimated by this procedure and, in fact, for most of the region, the 20 mode solution is not noticeably better than the 16 mode solution. In this case, 387 time steps were taken but the time increased significantly to 6.5 minutes.

In studying the flow around a plate, the assumption of similarity provides us with an explicit formula for determining the boundary layer thickness. For the cylinder, the flow is not a similarity flow and there is no such simple formula. Most references settle for graphical descriptions of the velocity profiles, which make it difficult to estimate the boundary layer thickness with any real degree of accuracy. Once again referring to Blasius' work as discussed in Schlichting, it can be estimated (if only crudely) that δ varies from slightly less than 2 near stagnation to about 3 near separation. Using the same device to invert von Mises' transform as discussed in section 5, we found our estimated boundary layer thickness to vary from 7.02 at 0.005 (near stagnation) to 3.64 at separation. Only the 16 mode case was considered in this calculation.

Finally, it is not necessary to use the inviscid flow for the external velocity profile, although it is the easiest case for comparing with classical results. Many publications however, have made use of experimentally determined distributions. Flow about the cylinder seems to depend somewhat strongly on the Reynold's number of the flow, with the critical value being approximately 6.7×10^5. Above this value, the flow behaves, at least in the decelerated region, fairly close to potential flow (which we considered here) but for values below the critical number the pressure minimum and separation will occur much earlier. Although such cases will not be taken up here, all that is really needed to apply these techniques would be an explicit representation of $U_1(x)$, for example, by means of a power series expansion.

Graph 4 - Stress Profiles about Cylinder.

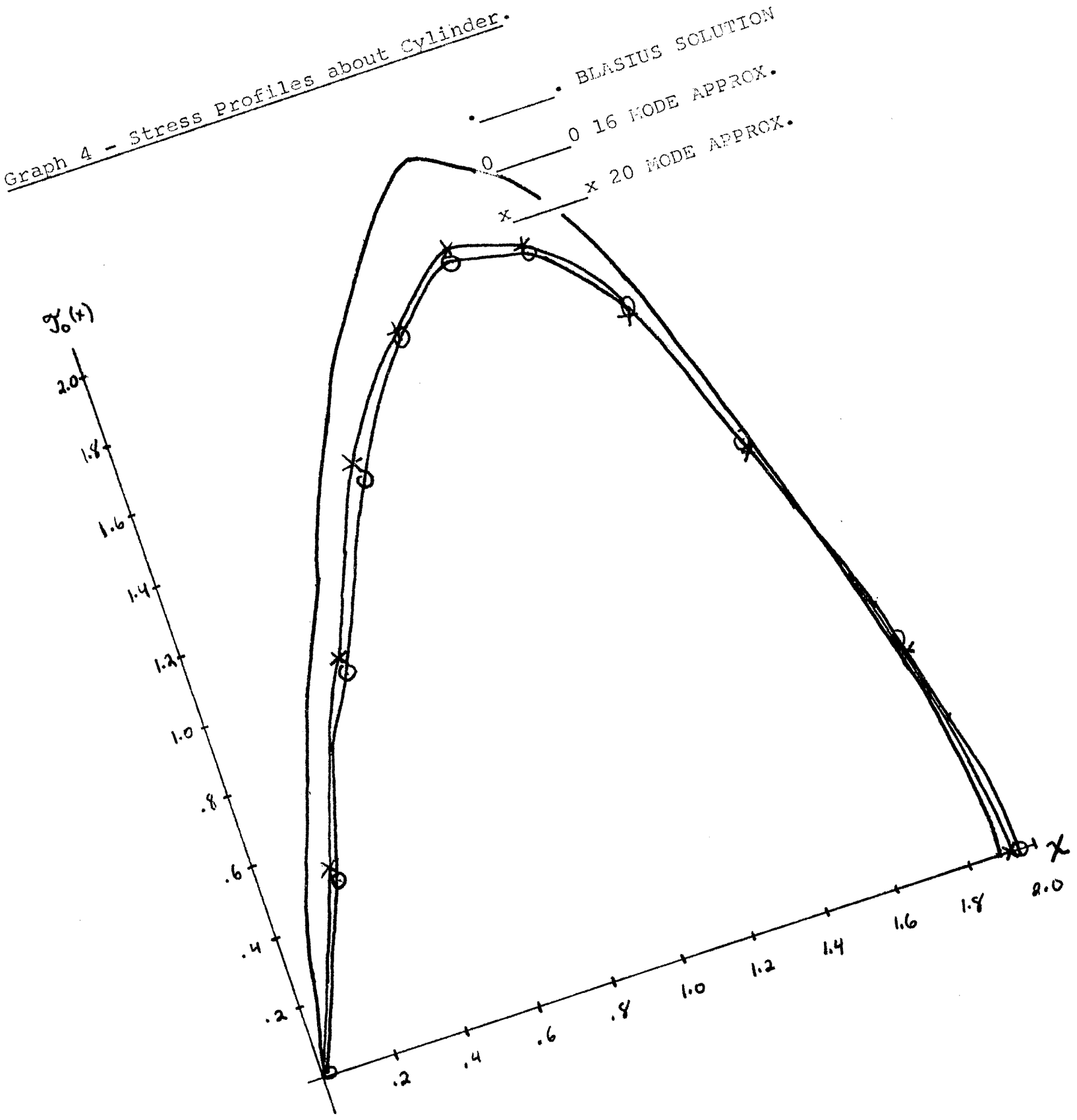

8. Linearly Retarded Flow.

By far the most disappointing results of this investigation were provided by the case of linearly retarded flow. The easiest description of this flow is that past a flat plate at zero incidence which abuts against a second plate perpendicular to the stream.

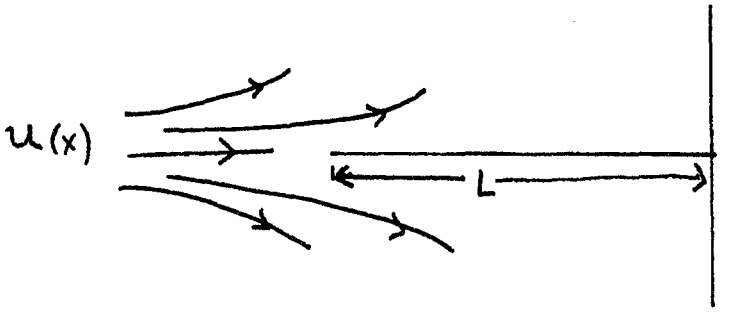

The external flow velocity is given by $U(x) = U_o(1-{}^{x}/L)$, where L represents the distance from the leading edge of the plate to the abutment point. The flow is obviously a generalization of ordinary plate flow; we therefore used the same initial profile as before.

The starting results are good and the error γ remains small throughout the process. However, the estimated point of separation is in gross error of what we should expect. Using the non-dimensional variable $x^* = {}^{x}/L$, classical results show that separation should occur at $x^* = 0.12$. The linear programming scheme, using 16 modes and 40 grid points in y (across the boundary layer), showed separation as occurring at $x^* = 0.193$. This represents an error of about 60%.

Our experience in the cylinder problem was that boosting the expansion up to 20 modes was not really very helpful. In an attempt to match the velocity profile to Prandtl's equation more closely, we instead repeated the 16 mode expansion, this time with 50 grid points taken across the boundary layer.

The results were still rather poor. The separation point is now located at about 0.183, this is still about 50% in error. Graph 5 compares the classical stress profile (based on Goldstein's calculations) with our 40 and 50 grid point expansions.

Graph 5 - Stress Profiles. Linearly Retarded Flow

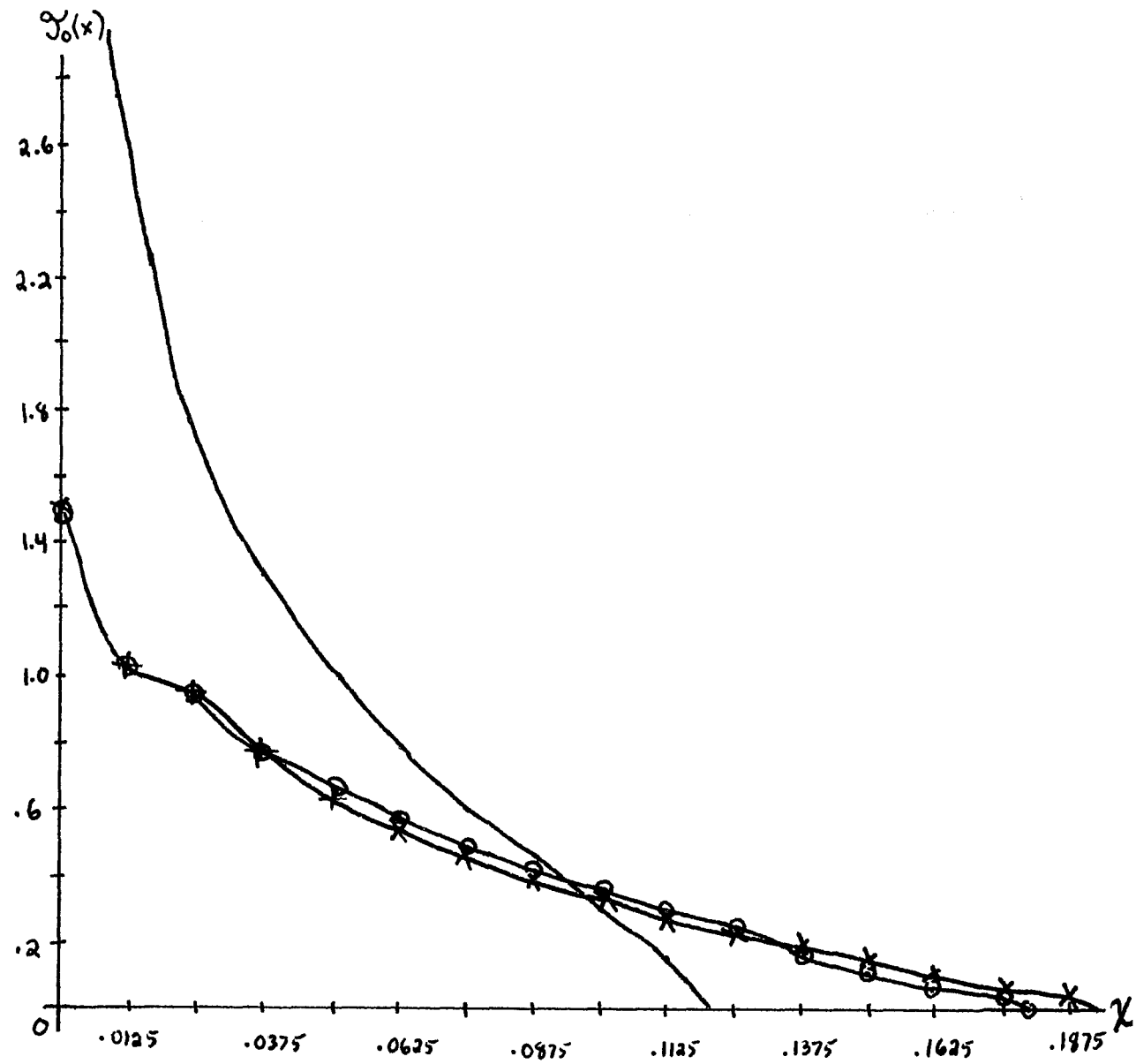

9. Some Final Conclusions.

The proposed linear programming technique was reasonably successful in two of our three test cases. To some extent, the difficulty in the method can be attributed to our relative naivete in handling the singularity at the wall. We simply did not demand that the series match the partial differential equation at the wall and instead demanding that the boundary condition be matched there. One possible way of rectifying this would be to consider an approximation which combined a series (such as the one we used here) with one or more auxilary functions. The role of these functions would be to match the initial profile, the external flow, or both and possibly to simulate the singularity at the wall.

The choice of the Chebyshev polynomials was not mandatory, although they do tend to form more rapidly converging series than other polynomials, for example, the Legendre polynomials. Experimenting with other sets of functions in the series expansion might have proved profitable but was not attempted in this investigation.

Within certain limits, the method seems to be a promising one. Modifications along the lines mentioned above probably will yield an even stronger model for a large class of incompressible boundary layer flows.

BIBLIOGRAPHY

1. G.K. Batchelor — "Introduction to Fluid Dynamics" Cambridge University Press (1967)

2. S. Goldstein (ed.) — "Modern Developments in Fluid Dynamics", Dover Publications, Inc. (1965)

3. C.E. Grosch and S.A. Orszag — Problems in Unbounded Regions: Co-ordinate Transforms J. Comp. Phys. p. 273-296 (1977)

4. G. Hadley — "Linear Programming" Addison-Wesley, Inc. (1966)

5. C.C. Hsu — A Galerkin Method for a Class of Steady, Two-Dimensional, Incompressible Laminar Boundary Layer Flows. J. Fluid Mech vol. 69 p. 783-802 (1975)

6. IMSL Manual — International Mathematics and Statistical Library User's Manual (1975)

7. K. Nickel — Prandtl's Boundary Layer Theory from the Viewpoint of a Mathematician Ann. Rev. Fluid Mech. p.405-428 (1977)

8. J.B. Rosen — Approximate Computational Solution of Non-Linear Parabloic Partial Differential Equations by Linear Programming "Numerical Solutions of Non-Linear Differential Equations" J. Wiley, and Sons, Inc. (1966)

9. H. Schlichting — "Boundary Layer Theory", Addison-Wesley, Inc. (1968)

10. J. Serrin — Asymptotic Behaviour of Velocity Profiles in the Prandtl Boundary Layer Theory Proc. Royal Soc. A 299 p. 491-507 (1967)